New Phytologist

Research

Double DJ-1 domain containing *Arabidopsis* DJ-1D is a robust macromolecule deglycase

Melvin Prasad[1]*, Priyanka Kataria[2]*, Sunayana Ningaraju[2], Radhika Buddidathi[1], Kondalarao Bankapalli[2], Chenna Swetha[1], Gautam Susarla[2], Radhika Venkatesan[1,3], Patrick D'Silva[2] and Padubidri V. Shivaprasad[1]

[1]National Centre for Biological Sciences, GKVK Campus, Bangalore 560 065, India; [2]Department of Biochemistry, Indian Institute of Science, C.V. Raman Avenue, Bangalore 560 012, India; [3]Department of Biological Sciences, Indian Institute of Science Education and Research Kolkata, Mohanpur, West Bengal 741246, India

Authors for correspondence:
Padubidri V. Shivaprasad
Email: shivaprasad@ncbs.res.in

Patrick D'Silva
Email: patrick@iisc.ac.in

Received: *11 May 2022*
Accepted: *13 July 2022*

New Phytologist (2022) **236:** 1061–1074
doi: 10.1111/nph.18414

Key words: advanced glycation end-products, *Arabidopsis thaliana*, DJ-1 family proteins, DNA repair, glycation, methylglyoxal, reactive carbonyls, stress responses.

Summary

- Plants, being sessile, are prone to genotoxin-induced macromolecule damage. Among the inevitable damaging agents are reactive carbonyls that induce glycation of DNA, RNA and proteins to result in the build-up of advanced glycated end-products. However, it is unclear how plants repair glycated macromolecules. DJ-1/PARK7 members are a highly conserved family of moonlighting proteins having double domains in higher plants and single domains in other phyla.
- Here we show that *Arabidopsis* DJ-1D offers robust tolerance to endogenous and exogenous stresses through its ability to repair glycated DNA, RNA and proteins. DJ-1D also reduced the formation of reactive carbonyls through its efficient methylglyoxalase activity. Strikingly, full-length double domain-containing DJ-1D suppressed the formation of advanced glycated end-products in yeast and plants.
- DJ-1D also efficiently repaired glycated nucleic acids and nucleotides *in vitro* and mitochondrial DNA *in vivo* under stress, indicating the existence of a new DNA repair pathway in plants.
- We propose that multi-stress responding plant DJ-1 members, often present in multiple copies among plants, probably contributed to the adaptation to a variety of endogenous and exogenous stresses.

Introduction

Genomes of all organisms are routinely challenged by endogenous or exogenous genotoxins such as ionizing radiation, ultraviolet (UV) rays and various chemicals (Cannan & Pederson, 2016; Chatterjee & Walker, 2017). The inevitable errors induced by these factors lead to modifications of nucleotides, intra- or interstrand cross-links, and breaks in phosphodiester bonds. Organisms have ready mechanisms to repair DNA to avoid complications in DNA organization, replication or transcription (Chatterjee & Walker, 2017). Being sessile, plants are more vulnerable to DNA-damaging factors. Nevertheless, they have evolved a complex network of flexible mechanisms of DNA damage detection and repair, ensuring genomic stability. Such mechanisms include the removal of DNA lesions and reconstitution of the original genetic information.

A major source of endogenous DNA lesions arises from intracellular metabolism which generates free radicals. Plants and algae are prone to photo-oxidative stress as a result of the build-up of reactive oxygen species (ROS) generated during photosynthesis. Several types of ROS are generated at various sites, especially in the chloroplast and mitochondria, with influencing factors such as light, temperature, drought, nutrient deficiencies and biotic factors. Reactive oxygen species can damage many cellular constituents, including lipids, proteins, pigments and DNA (Xie *et al.*, 2019). When ROS reacts with DNA, the most frequently generated lesion is 7,8-dihydro-8-oxoguanine (8-oxo-G), which is highly mutagenic (Atamna *et al.*, 2000). Another equally important lesion is the glycation of DNA, when reactive carbonyls such as glyoxal (GO) and methylglyoxal (MG) react with DNA to produce aminocarbinols and advanced glycated end-products (AGEs) such as cyclic imidazopurinones (Thornalley *et al.*, 2010). These reactive carbonyls are by-products of glycolysis generated in all living cells, often specifically glycating guanosines (G) and deoxyguanosines (dG) in nucleic acids. Thornalley (2008) measured cellular concentrations of 8-oxo-G and glycated dG and found that they accumulate at similar concentrations, indicating the significance of glycation in DNA damage.

Common downstream effects of DNA glycation are not very different from those of 8-oxo-G, which includes increased mutations, strand breaks, cytotoxicity and tumorigenesis as observed

*These authors contributed equally to this work.

in animals (Richarme *et al.*, 2017). In all studied organisms, oxidized DNA or nucleotides are repaired through a well-known guanine oxidation repair system; however, a dedicated system for the repair of glycated DNA was reported only recently. Richarme *et al.* (2017) identified a family of deglycases called DJ-1 family Maillard deglycases as major repair systems in bacteria and animals. Moreover, the deglycase activity of human DJ-1 (hDJ-1/PARK7) was harnessed to alter the epigenetic landscape and to disaggregate glycated proteins (Sharma *et al.*, 2019; Zheng *et al.*, 2019). Besides hDJ-1 and bacterial DJ-1, *Plasmodium falciparum* DJ-1 (*Pf* DJ-1) was also shown to possess deglycase activity (Nair *et al.*, 2018). Human PARK7 and yeast Hsp31 are well-characterized DJ-1 homologs that detoxify MG and protect cells from various stresses (Davie, 2008; Bankapalli *et al.*, 2015). In addition, several DJ-1 members have been implicated in diverse cellular processes, such as transcriptional regulation, quenching ROS, regulation of signal transduction pathways, protein folding and modulation of glucose concentrations (Miller-Fleming *et al.*, 2014; Cao *et al.*, 2015; Tsai *et al.*, 2015).

As a high rate of photosynthesis in optimal conditions can produce huge amounts of reactive carbonyls in plants, they are particularly prone to glycation damage (Shimakawa *et al.*, 2014). Although plants have robust methylglyoxalase activities to remove the reactive carbonyls, it is not known how plants cope with glycated DNA and proteins.

Here we show that a plant DJ-1 member is able to remove build-up of MG as well as act as a repair hub for glycated DNA, RNA and protein macromolecules. In yeast, plant DJ-1D complemented Glyoxalase I (Δ*glo1*) deleted strain under MG stress, indicating its methylglyoxalase activity. Purified and transgenically expressed DJ-1D offered stress tolerance by efficiently deglycating proteins and nucleic acids to inhibit the formation of AGEs. DJ-1D was relocalized into the mitochondria to prevent and actively repair damage to DNA under stress. In summary, our data highlight the presence of double domains in plant DJ-1D, which enables a superior response to neutralize various stresses and to avoid build-up of toxic by-products of unavoidable glycolysis as compared with single-domain orthologs.

Materials and Methods

Plant materials, growth conditions and plant transformation

Wild-type (WT) *Arabidopsis thaliana* (L.) Heynh. plants of Columbia (Col-0) ecotype plants were grown at 16 h : 8 h, light : dark (22°C) and a photon flux density of 150–170 μE m^{-2} s^{-1}, at 70% humidity. *Nicotiana tabacum* L. cv Wisconsin 38 plants were raised on agar-solidified Murashige & Skoog (MS) medium (Murashige & Skoog, 1962) containing 30 g l^{-1} sucrose. Tobacco plants were maintained in the tissue culture room with 200 mmol photons m^{-2} s^{-1}. Transformation of tobacco was performed as described previously (Shivaprasad *et al.*, 2006). Transgenic plants were regenerated from kanamycin-resistant calli. Transgenic *Arabidopsis* were generated through the floral dip method (Zhang *et al.*, 2006).

Sequence alignment and phylogenetic analysis

Multiple sequence alignment (MSA) was performed using ClustalW, after which MSA files were manually edited and visualized by ESPript 3.0. The phylogenetic analysis was carried out using a maximum likelihood algorithm and a phylogenetic tree was constructed with Mega using 100 bootstrap replications.

Plasmid constructs, yeast strains and genetic analysis

The haploid yeast BY4741 (*MATa his3Δ1 leu2Δ0 met15Δ0 ura3Δ0*) used here was obtained from Open Biosystems (Huntsville, AL, USA). Haploid Δ*hsp31* strain was generated by homologous recombination as previously described (Bankapalli *et al.*, 2015). Δ*glo1* and Δ*sod1* strains were generated by homologous recombination using a PCR product containing *hphNT1* cassette and flanking sequences of glyoxalase1 and superoxide dismutase 1 (SOD1) loci, respectively. *Arabidopsis thaliana* DJ-1D was cloned into pRS415 using *Bam*HI and *Sal*I sites. m1 and m2 were cloned separately in pRS415 vector under translational elongation factor (TEF) and glyceraldehyde-3-phosphate dehydrogenase (GPD) promoters with an N-terminal hemagglutinin (HA)-tag using primers listed in Supporting Information Table S1. Mutations in DJ-1D and SOD1 were generated by PCR-based site-directed mutagenesis using suitable primers (Table S1). For protein purification, DJ-1D and its mutants were cloned into pRSF-duet vector. However, m1 and m2 were cloned in the pRSET-C vector. SOD1 H46R mutant was cloned into pRS426 under a GDP promoter.

For plant transformation, binary plasmid pBIN-HSP31 (Melvin *et al.*, 2017) was replaced with DJ-1D or its mutants. For the preparation of DJ-1D_eGFP fusion construct, DJ-1D was cloned next to eGFP (pBIN-ScHsp31-eGFP; Melvin *et al.*, 2017; Table S1). Other mutations in DJ-1D (m3, m4, m5, m7) were generated by PCR-based site-directed mutagenesis using the Quick-Change method (Stratagene, San Diego, CA, USA). Products were cloned into pRS415 vector and mutations were confirmed by sequencing.

Phenotypic analysis

Yeast strains were grown overnight in synthetic dropout media harvested at the mid-log phase (A_{600} ~ 0.6). For oxidative stress, cells were resuspended in sterile water and treated with 1.5 mM H_2O_2 followed by incubation at 30°C for 2 h. Subsequently, cells were washed with sterile water, serially diluted with 10-fold difference and spotted on synthetic dropout media. Plates were incubated at 30°C. For methylglyoxal stress, cells were pelleted down at the mid-log phase and spotted on synthetic dropout media with or without 0.5 mM methylglyoxal (M0252; Sigma). Δ*sod1* strains expressing the hSOD1 H46R mutant and DJ-1D were grown until the mid-log phase and spotted on synthetic dropout media. The plates were incubated at different temperatures.

Leaf disk Chl retention assay

Leaf disk assay was performed as described previously (Veena *et al.*, 1999). Briefly, leaves were floated in ½MS medium

supplemented with or without an appropriate concentration of stress inducers (all concentrations were previously calibrated). These experiments were repeated three times with three biological replicates.

Estimation of MG and MDA measurements

Accumulation of MG and MDA were quantified according to the methods described in Melvin *et al.* (2017).

In vitro deglycation assay

For the protein deglycation assay, SOD1 (1.5 μg) and lysozyme (1.5 μg) were incubated with 2 mM MG in 50 mM sodium phosphate buffer at 37°C for 2 h after which DJ-1D proteins (5 μg) were added to the reaction mixture and incubated for 4 h. Subsequently, the samples were separated using sodium dodecyl sulfate-polyacrylamide gel electrophoresis (SDS-PAGE), and western analysis was performed using Anti-MAGE antibody (ab243074; Abcam, Cambridge, UK), which is specific for arg-pyrimidine (Intermediate for methylglyoxal modification).

For the DNA deglycation assay, *c.* 500 μM of GTP or dGTP was incubated at 37°C in 50 mM sodium phosphate buffer (pH 7.0), without or with 5 mM MG for 15 h, and afterwards DJ-1D proteins were added to the reaction mixture. The samples were analyzed by reversed-phase high-performance liquid chromatography (RP-HPLC) on a C18 RP-HPLC Symmetry Column (5 μm Spherical Silica, 4.6 mm × 150 mm, Shimadzu Prominence-i, Kyoto, Japan) equilibrated in 100 mM potassium phosphate buffer (pH 5.5) at 22°C, and eluted with the same buffer.

For the PCR-based DNA assay, forward and reverse PCR primers (8 μM each) of tobacco NADH dehydrogenase (forward, TTGCGGATCCATGATACTTTCTGTTTTGTCG; reverse, TTTCGAGCTCTTAATAGCATTTATCGATGC) or ATP synthase (forward, TTGCGGATCCATGTTTCGACGTATAT TTTTATTTG; reverse, TTTCGAGCTCTTGATGAAGATTT ATAGCATC) were incubated at 37°C for 2 h in 50 mM sodium phosphate (pH 7.0) buffer containing 5 mM MG. Afterwards, purified DJ-1D and its mutant proteins (5 μg) were added to the glycation mixture. Treated primers were separated from MG using QIAquick nucleotide removal kit (Qiagen) and subjected to PCR.

In vitro disaggregation assay

Bovine liver rhodanese (Sigma) was used as a model substrate to analyze the aggregation prevention activity of DJ-1D using an established protocol (Goswami *et al.*, 2010). Rhodanese was denatured in 6 M guanidine hydrochloride and diluted in reaction buffer. Aggregation of rhodanese (0.46 μM) in the presence or absence of DJ-1D (4.6 μM) was monitored against the change of absorbance with different time intervals at 320 nm. Bovine serum albumin (BSA) was used as a negative control.

Fluorescence analysis of glycated RNA

RNA deglycation activity assays were performed as previously described (Richarme *et al.*, 2017) with modifications. Total RNA (5 μg) prepared from *Sacharomyces cerevisea* was incubated for 12 h at 37°C in 50 mM sodium phosphate buffer (pH 7.0) containing 5 mM MG. Subsequently, DJ-1D and m7 were added to the reaction mixture and further incubated for 6 h. Fluorescence was measured between 400 and 500 nm using a Jasco FP 6300 spectrofluorometer (Tokyo, Japan).

Purification of mitochondria

The leaves from transgenic DJ-1D-overexpressed plants were treated with or without 5 mM H_2O_2 and subjected to mitochondrial isolation. Leaves were ground in grinding buffer (0.3 M sucrose; 2 mM EDTA; 10 mM KH_2PO_4; 25 mM tetrasodium pyrophosphate; 1% polyvinylpyrrolidone (PVP-40); 1% BSA; 20 mM ascorbate, pH 7.5) into a homogenous suspension and filtered through four layers of gauze. Later, the extract was centrifuged at 2400 ***g*** for 5 min at 4°C to remove cell debris and other organelles. The supernatant was centrifuged at 17 000 ***g*** for 20 min at 4°C to pellet down mitochondria and thylakoids. The pellet was resuspended in washing buffer (0.3 M sucrose; 10 mM N-Tris(hydroxymethyl)methyl-2-aminoethane sulphuric acid pH 7.5; 0.1% BSA) and centrifuged at 2400 ***g*** for 5 min at 4°C to remove any remaining chloroplasts. The supernatant was centrifuged at 17 400 ***g*** for 20 min at 4°C to pellet down mitochondria and then resuspended in washing buffer. Subsequently, it was loaded onto PVP-40 gradients (0–4.4% PVP in 28% Percoll in washing buffer) and centrifuged at 40 000 ***g*** for 40 min at 4°C without brake. The mitochondria obtained were washed in washing buffer and pelleted at 31 000 ***g*** for 15 min at 4°C.

Isolation of nuclei

Isolation of nuclei was performed by using an established protocol as previously described (Song *et al.*, 2016).

Analysis of mitochondrial genes

Total DNA was isolated from tobacco using cetyltrimethyl ammonium bromide (Xin & Chen, 2012), which was used as a template to amplify *Nt*NDH2, *Nt*COX1, *Nt*MRP and *Nt*DPH using appropriate primers (Table S2). PCR products were gel eluted and purified using the QIAquick Gel Extraction Kit (Qiagen) and libraries were prepared using the Nextera XT DNA Library Prep Kit (Illumina) and sequenced in a 1 × 50 bp run on HiSeq 2500. The obtained reads were trimmed for low quality and adapters. The filtered reads were aligned to the mitochondrial genes from each sample using Bowtie (v.1) with zero mismatches. The DNA mutation was calculated as the total number of nucleotides with mismatch threshold > 10% corresponding to the reference gene sequence divided by the total length of the gene.

Quantification and statistical analysis

Band intensity quantification was performed using ImageJ. Statistical analyses were performed using GraphPad Prism 6.0. Error

bars represent SE and are derived from a minimum of three replicates. For significance testing by one-way ANOVA, Dunnett's multiple comparison post-test was used. Asterisks represent the following significance values: *, $P \leq 0.05$; **, $P \leq 0.01$; ***, $P \leq 0.001$; ****, $P \leq 0.0001$.

Refer to Methods S1–S6 for details on the RNA extraction and quantitative reverse transcription polymerase chain reaction (qRT-PCR) analysis, protein purification and immunoblotting, methylglyoxalase activity assay, DAB staining for H_2O_2, transient expression and subcellular localization of DJ-1D and measurement of ROS concentrations.

Results

Arabidopsis DJ-1D is a novel methylglyoxalase with functionally redundant duplicate domains

Human PARK7 and yeast Hsp31 are well-characterized DJ-1 homologs that detoxify MG and protect cells from various stresses (Davie, 2008; Bankapalli *et al.*, 2015). DJ-1 members are also implicated in diverse cellular processes, such as transcriptional regulation, quenching ROS, regulation of signal transduction pathways, protein folding and modulation of glucose concentrations (Cao *et al.*, 2015). Intriguingly, plant homologs of DJ-1 are unlike those of animals, yeast and bacteria, often twice their size, sharing few homologies with their animal counterparts (Fig. S1). Surprisingly, domain fusion in plant homologs might have arisen among ancestors of algae, as some algae have single domains as in bacteria and animals, whereas few others have double domains (Figs S1a,b, S2). Plants also have multiple copies of DJ-1 members, unlike animals, where they are usually single-copy genes. Copies of DJ-1 proteins in monocots (ranging between 6 and 21) are higher than among dicots (3–11; Table S3). Double domains in plant DJ-1 homologs probably arose as a result of a gene duplication-fusion event which is often recognized as a powerful source of genetic novelty, morphological diversity and speciation (Panchy *et al.*, 2016). It is interesting as to why exactly DJ-1 proteins have undergone such changes. Six isoforms of DJ-1 proteins (DJ-1A, DJ-1B, DJ-1C, DJ-1D, DJ-1E and DJ-1F) have been identified in the model plant *Arabidopsis* (Kwon *et al.*, 2013). Among these, DJ-1D, DJ-1E and DJ-1F formed a separate clade with individual domains having conserved cysteine (Cys) and histidine (his) residues similar to yeast Hsp31 and *E. coli* YhbO (YhbO/PfpI clade), whereas the remaining DJ-1 members clustered separately (Figs 1a, S2). Plant DJ-1 members had two almost identical domains and twice the size of bacterial, yeast and human DJ-1 members (Figs 1b, S1a,b, S3a). We analyzed the expression profiles of *Arabidopsis* DJ-1 homologs in various tissues and observed that DJ-1A, DJ-1B and DJ-1D are expressed abundantly across all the tested tissue samples (Fig. S3b; Methods S1). *Arabidopsis* DJ-1 members have varying degrees of methylglyoxalase activities *in vitro* (Kwon *et al.*, 2013), and they are associated with chloroplast development (Lin *et al.*, 2011) and cell death (Xu *et al.*, 2010); however, specific functions of plant DJ-1 isoforms are unknown.

DJ-1D forms a subclade (Fig. 1a) with two domains which shares homology with *Saccharomyces cerevisiae* Hsp31 and human PARK7 (Fig. S3a,c). In PARK7 and Hsp31, conserved Cys residues in the catalytic triad are required for protecting cells from metabolic stresses (Subedi *et al.*, 2011; Lee *et al.*, 2012; Bankapalli *et al.*, 2015), and such motifs are duplicated in DJ-1D as a result of the presence of a double domain (Lin *et al.*, 2011). We generated Cys and His residue mutants in both N- and C-terminal ends, as well as truncated versions with either the N- or C-terminal bits with one DJ-1 domain alone for functional analysis (Fig. 1b). To investigate the functional significance of

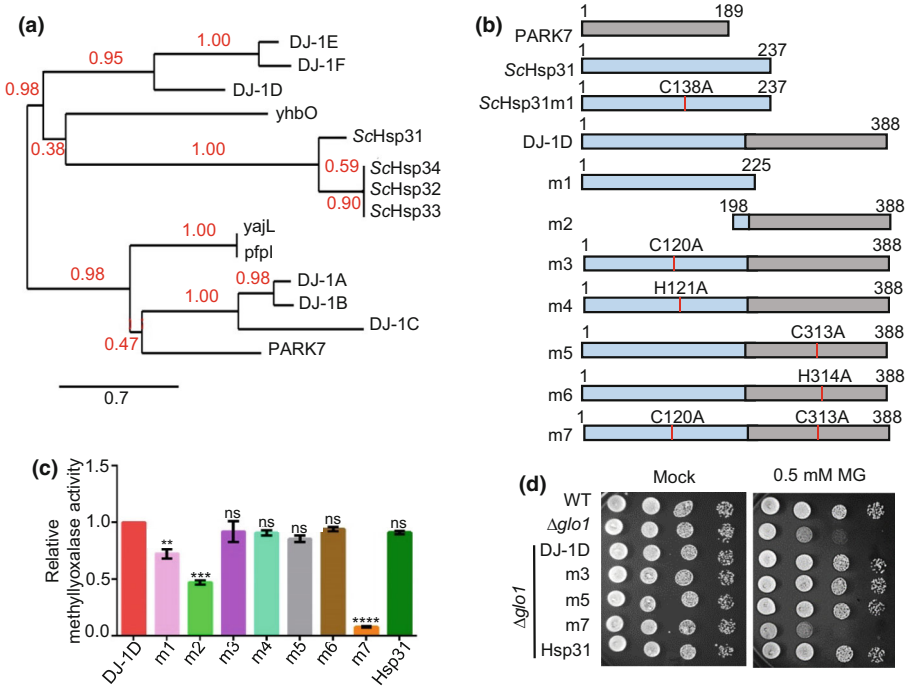

Fig. 1 *Arabidopsis* DJ-1D is a novel methylglyoxalase with functionally redundant duplicate domains. (a) Phylogenetic tree showing close relatives of *Arabidopsis* DJ-1. ClustalW alignments were used for a maximum-likelihood tree with 100 bootstrap replications. Bootstrap values are shown in red. (b) Domain structure of DJ-1D. N- and C-terminal pfpI/DJ-1 domains are marked in different colors, and positions of mutations are indicated. A, alanine; C, cysteine; H, histidine. (c) *In vitro* measurement of methylglyoxalase activity at 24°C. *Sc*Hsp31 served as a positive control. Data from three representative experiments are shown (mean ± SE; one-way ANOVA: *, $P \leq 0.05$; **, $P \leq 0.01$; ***, $P \leq 0.001$; ****, $P \leq 0.0001$; ns, not significant, in comparison to the wild-type (WT)). (d) Growth phenotype analysis of DJ-1D$_{WT}$ and its mutants in *Saccharomyces cerevisiae* BY4741. Spot analysis was carried out with 10-fold dilution on SD Leu$^-$ medium with 0.5 mM methylglyoxal (MG). Images were captured after 36 h of growth at 30°C.

DJ-1D in plants, we initially purified histidine-tagged DJ-1D and its mutants using Ni^{2+}NTA affinity chromatography from *E. coli* (Fig. S4a; Methods S2) and subjected them to a methylglyoxalase activity assay as previously described (Bankapalli *et al.*, 2015). The activity shown by the DJ-1D protein was moderately greater than that of its ortholog, *S. cerevisiae* Hsp31 (Figs 1c, S4b; Methods S3). Further, the N-terminal domain (m1) and C-terminal domain (m2) alone also exhibited methylglyoxalase activities, but to a lesser extent than DJ-$1D_{WT}$ at 24°C. However, the C-terminal domain (DJ-1Dm2) showed a cessation of its methylglyoxalase activity as compared with the WT and DJ-1Dm1 at higher temperatures (Fig. S4c–e). This difference might be a result of a better protein stability of the truncated domain at lower temperatures. Point mutations in Cys and His residues that abolish or reduce activities of Hsp31 or PARK7 did not abolish methylglyoxalase activities in full-length DJ-1D in either N- (m3, m4) or C-terminal (m5 and m6) versions. Conversely, the double mutant that carries mutation in both the domains (DJ-1Dm7) showed a complete abrogation in its methylglyoxalase activity at all the tested temperatures. This finding shows that both domains are functional; however, the full-length double domain has greater stability and higher activity.

Based on these findings, we further tested the role of plant DJ-1D and its mutants in combating MG toxicity *in vivo*, using the *S. cerevisiae* model system. We deleted *glo1* which encodes glyoxalase-I, a key enzyme responsible for detoxification of glyoxals in BY4741 background. DJ-1D and its mutants were expressed under the TEF promoter in the Δ*glo1* strain and subjected to growth phenotype analysis. Not surprisingly, the Δ*glo1* strain displayed severe growth sensitivity when grown in agar media containing 0.5 mM MG, in comparison to the WT (Fig. 1d). On the other hand, owing to their robust *in vitro* methylglyoxalase activity, overexpression of DJ-1D, m3, m5 complemented the growth of Δ*glo1* on MG-containing media. However, m7, which lacks detectable methylglyoxalase activity, was unable to restore the growth phenotype of the Δ*glo1* strain (Fig. 1d). To rule out the possibility that the observed growth phenotype was not a result of expression levels of DJ-1 members, we analyzed the steady-state abundance of the proteins using anti-HA antibody and confirmed that the expression of all mutants was at WT DJ-1D levels (Fig. S4f; Methods S2). Together, our results indicate the indispensability of both the domains in DJ-1D in protecting cells against MG stress, which is higher than single domain-containing deletion mutants or *Sc*Hsp31.

DJ-1D attenuates the formation of advanced glycation end-products

Elevated concentrations of methylglyoxal are associated with enhanced protein glycation, hampering their ability to function *in vivo* (Ahmed *et al.*, 2003). As DJ-1D exhibited methylglyoxalase activity, it was imperative for us to evaluate whether DJ-1D can reduce AGE levels *in vivo*. To test this, WT (BY4741), Δ*glo1*, Δ*glo1*/DJ-1D and Δ*glo1*/m7 yeast strains were grown until the mid-log phase and subjected to 2 mM MG stress. Subsequently, the cell lysates were subjected to western analysis using anti-AGE and anti-MAGE (MG-induced AGEs) antibodies. As expected, the Δ*glo1* strain had enhanced AGE formation in comparison to the WT as a result of increased concentrations of MG (Fig. 2a,b). Interestingly, the expression of DJ-1D in Δ*glo1* significantly suppressed AGE levels. By contrast, the expression of m7 was defective in lowering the formation of AGEs (Fig. 2a,b). In agreement with these observations, concentrations of MG-induced AGEs were also reduced in cells expressing DJ-1D as seen upon probing with anti-MAGE antibody (Fig. 2b). Reduced accumulation of AGEs might be a result of reduced MG concentrations. Recent studies have shown that DJ-1 proteins from bacteria and humans perform protein deglycation by removing sugars from cysteine, arginine and lysine residues of proteins (Richarme *et al.*, 2015; Abdallah *et al.*, 2016). As protein deglycase functions of plant homologs are unknown, we explored whether *Arabidopsis* DJ-1D has deglycase activity. Two protein substrates, namely, SOD1 and lysozyme, were incubated with 2 mM MG in individual reactions. After the modification of substrates with MG, the DJ-1D and mutants were added to the reaction mixture in equimolar concentrations. The glycation and deglycation statuses of the substrates were determined by performing western analysis using Anti-MAGE antibody. The addition of DJ-1D, m3 and m5 to the reactions showed a significant reduction in the glycated bands of SOD1 and lysozyme (Fig. 2c,d). However, in agreement with the previous observations *in vivo*, addition of m7 was unable to reduce MG-induced AGE formation. According to a previous study, hDJ-1 was shown to perform deglycation by its chaperoning activity to allow binding and to gain access to glycated macromolecules (Richarme *et al.*, 2015). In a similar line, we examined the chaperone activity of DJ-1D *in vivo* by utilizing a well-reported mutant of SOD1, which is known to aggregate and induce amyotrophic lateral sclerosis (ALS) in humans. The overexpression of hSOD1 H46R in *S. cerevisiae* (Δ*sod1* strain) at different temperatures displayed growth sensitivity (Fig. 2e). At the same time, the viability was significantly enhanced in the presence of DJ-1D, presumably by lowering SOD1-mediated toxicity through its chaperoning function (Fig. 2e). To measure chaperone activity quantitatively *in vitro*, we performed *in vitro* rhodanese disaggregation assay. The rhodanese, alone or in the presence of BSA (control), showed robust aggregation as monitored by time-dependent changes in the absorbance at 320 nm (Fig. 2f). However, addition of DJ-1D (1 : 10 ratio) showed significant protection against aggregation of rhodanese, thus highlighting the disaggregase chaperoning activity of the DJ-1D protein, consistent with our *in vivo* observations. In conclusion, our *in vivo* and *in vitro* results highlight the role of DJ-1D in preventing the formation of AGEs by repairing glycated proteins through its robust chaperoning activity.

DJ-1D repairs MG-induced DNA glycation

PARK7 and bacterial DJ-1 are recently discovered novel deglycases that repair the DNA damage induced by MG (Richarme *et al.*, 2017). Guanine (G) residue reacts with MG and forms

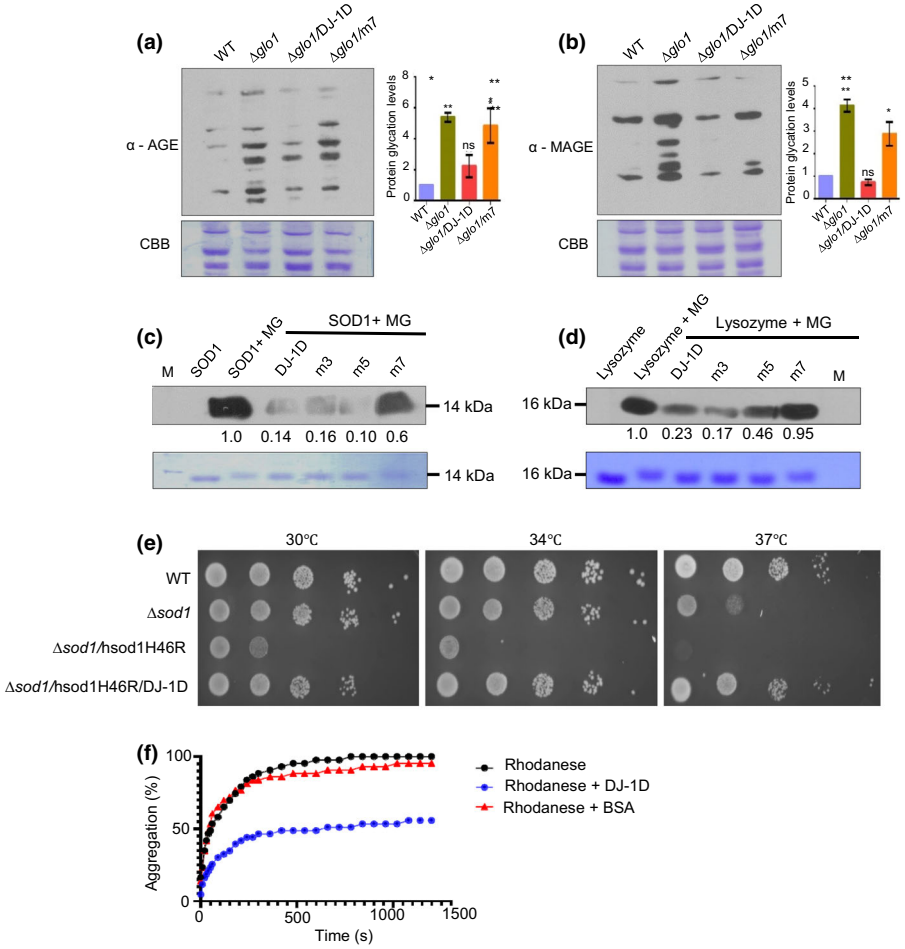

Fig. 2 DJ-1D attenuates advanced glycated end-product (AGE) formation and exhibits protein deglycase activity. (a, b) Cells from different yeast strains were treated with 1 mM methylglyoxal (MG) for 3 h. Lysates were separated on sodium dodecyl sulfate–polyacrylamide gel electrophoresis (SDS-PAGE) and detected by western blotting using anti-AGE (a) and anti-MG glycated AGE (MAGE) (b) antibody. Data from three representative experiments are shown (mean ± SE; one-way ANOVA: *, $P \leq 0.05$; **, $P \leq 0.01$; ns, not significant). Coomassie blue-stained gel served as loading control. (c, d) SOD1 and lysozyme were incubated separately with MG at 37°C for a brief period, and afterwards DJ-1D$_{WT}$ and mutants were added to the reaction mixture and western analysis was done with anti-MAGE antibody. Analysis of chaperone activity of DJ-1D. (e) DJ-1D rescues from hSOD1 mutant-mediated toxicity in yeast cells. SOD1 was deleted from the wild-type (WT, BY4741) strain of *Saccharomyces cerevisiae* and human SOD1 H46R mutant was overexpressed in pRS-425$_{GPD}$. Further, DJ-1D$_{WT}$ was overexpressed in Δ*sod1*/hsod1H46R strain and all the strains were subjected to phenotypic analysis. Plates were incubated at different temperatures (30, 34 and 37°C) and images were captured at 36 h. (f) DJ-1D prevents *in vitro* aggregation of rhodanese. Rhodanese was denatured in 6 M guanidine hydrochloride and diluted in reaction buffer. Absorbance change at 320 nm was used to monitor rhodanese (0.46 μM) aggregation with or without DJ-1D (4.6 μM) at different time intervals.

aminocarbinol, cyclic imidazopurinones and carboxyethyl-deoxyguanosine derivatives. Glycated DNA is not recognized by polymerases, resulting in error-prone replication that indicates the extent of damage to DNA. To assess whether DJ-1D can attenuate the formation of nucleotide AGEs (nAGEs), we incubated nucleotides (ATP, dATP, CTP, dCTP, dTTP, GTP, or dGTP) with MG for 15 h and analyzed products using RP-HPLC. As expected, MG did not react with nucleotides such as ATP, dATP, CTP, dCTP or dTTP and the products were eluted as single peaks (Fig. S5a–e; Table S4). However, incubation of MG with G (dGTP or GTP) formed glycated guanosine adducts, separating into six elution peaks for dGTP (Fig. 3a; Table S5) and five for GTP (Fig. 3b). These results matched observations made previously with animal DJ-1 proteins (Richarme *et al.*, 2017). Strikingly, in the presence of DJ-1D or its mutants m1, m3, m4 or m5, MG-were not detected, indicating active deglycation (Figs 3a,b, S5f). DJ-1Dm7 did not rescue the glycation of dGTP or GTP, forming multiple peaks similar to BSA control (Figs 3a,b, S5g). To verify if DJ-1D is indeed a deglycase rather than acting as a strong methylglyoxalase to remove MG during the glycation reaction, we added reaction components sequentially. We first incubated dGTP or GTP with MG for 12 h, and subsequently supplemented DJ-1D. Remarkably, adduct formation decreased over time, indicating active deglycation (Fig. 3c,d).

To further ascertain deglycation mediated by DJ-1D, forward and reverse primers of *N. tabacum* NADH dehydrogenase (NADH) and ATPase (ATP) genes were treated first with MG for 2 h and subsequently incubated with purified DJ-1D proteins before subjecting them to PCR amplification. In the absence of MG, both the genes were efficiently amplified. On the other

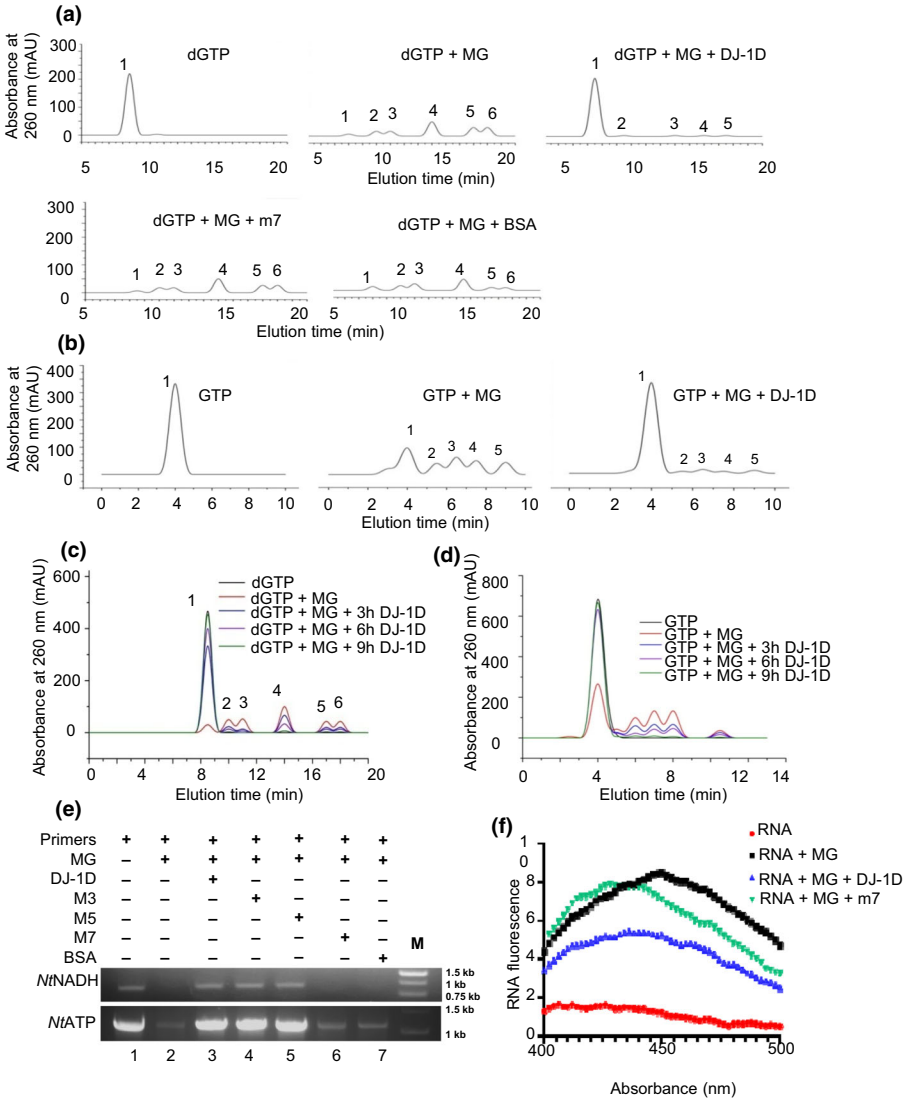

Fig. 3 DJ-1D repairs methylglyoxal (MG)-induced nucleic acid glycation. (a–d) Reversed-phase high-performance liquid chromatography (RP-HPLC) analysis of glycated nucleotides. (a) Approximately 500 μM of dGTP incubated with or without MG (5 mM) at 37°C in 50 mM sodium phosphate buffer (pH 7.0) for 12–16 h in the absence or presence of DJ-1D, m7 or bovine serum albumin (BSA) protein in the glycation mixture. (b) Approximately 500 μM of GTP incubated with or without MG (5 mM) at 37°C in 50 mM sodium phosphate buffer (pH 7.0) for 12–16 h in the absence or presence of DJ-1D protein. Samples were collected after 12 h and analyzed by RP-HPLC on a C18 RP-HPLC. (c, d) Approximately 500 μM dGTP (c) and GTP (d) were incubated at 37°C with or without 5 mM MG for 3, 6 and 9 h, and purified DJ-1D was subsequently added to the reaction mixture and samples were analyzed by RP-HPLC on a C18 RP-HPLC. Data are from three independent experiments. (e) PCR-based analysis of DNA deglycation activity of DJ-1D. Primers were incubated at 37°C for 2 h in 5 mM MG followed by the addition of 5 μM each of purified DJ-1D and its mutant proteins. Treated primers were purified and used for the PCR reaction. (f) RNA deglycation. Approximately 5 μg of total RNA was incubated with MG for 12 h, and afterwards DJ-1D, m7 and BSA were added to the reaction mixture. RNA glycation was analyzed by measuring its fluorescence between 400 and 500 nm.

hand, the addition of MG resulted in glycation of primers, leading to low amplification of PCR products (Fig. 3e, compare lanes 1 and 2). At the same time, the addition of DJ-1D (WT), m3, m4 and m5 to glycated primers was able to deglycate DNA efficiently, leading to amplification of both the genes to a similar level compared with the control treatment (Fig. 3e, compare lanes 1 with 3–5). However, the m7 mutant had low amplification to a similar level as the BSA-negative control (Fig. 3e, compare lanes 2 with 6–7). To test whether DJ-1D can also repair glycated RNA, we extracted total RNA from *S. cerevisiae* and treated it with MG for 16 h. RNA exhibits more fluorescence at 400–500 nm after glycation modifications than untreated controls (Fig. 3f). The addition of DJ-1D significantly reduced fluorescence intensity as a result of deglycation of RNA. On the other hand, the mutant m7 was incapabale of deglycating the RNA, thus retaining fluorescence similar to glycated RNA concentrations (Fig. 3f). These results highlight the fact that DJ-1D is a novel nucleic acid deglycase that can revert glycated DNA and RNA products into their native functional forms.

Expression of DJ-1D suppresses the oxidative stress phenotype in Δ*hsp31*

The elevated concentrations of MG are associated with increased oxidative stress; hence, we evaluated the role of DJ-1D in the maintenance of cellular redox homeostasis as observed for other DJ-1 members (Skoneczna *et al.*, 2007; Bankapalli *et al.*, 2015; Oh & Mouradian, 2018). To test this hypothesis, we utilized the Δ*hsp31* yeast strain which exhibits compromised growth phenotype under oxidative stress (Bankapalli *et al.*, 2015). Growth phenotype analysis was performed using the Δ*hsp31* strain transformed with DJ-1D and its mutants. Upon treatment with 1.5 mM H_2O_2, DJ-1D-transformed cells showed a significant growth restoration of Δ*hsp31* to the WT level (Fig. 4a). By contrast, m1 and m2 failed to suppress the growth sensitivity under H_2O_2 stress (Fig. S6a). The inability of m1 and m2 to restore the growth attributed to lower steady-state protein levels when expressed under the TEF promoter as compared with the WT as

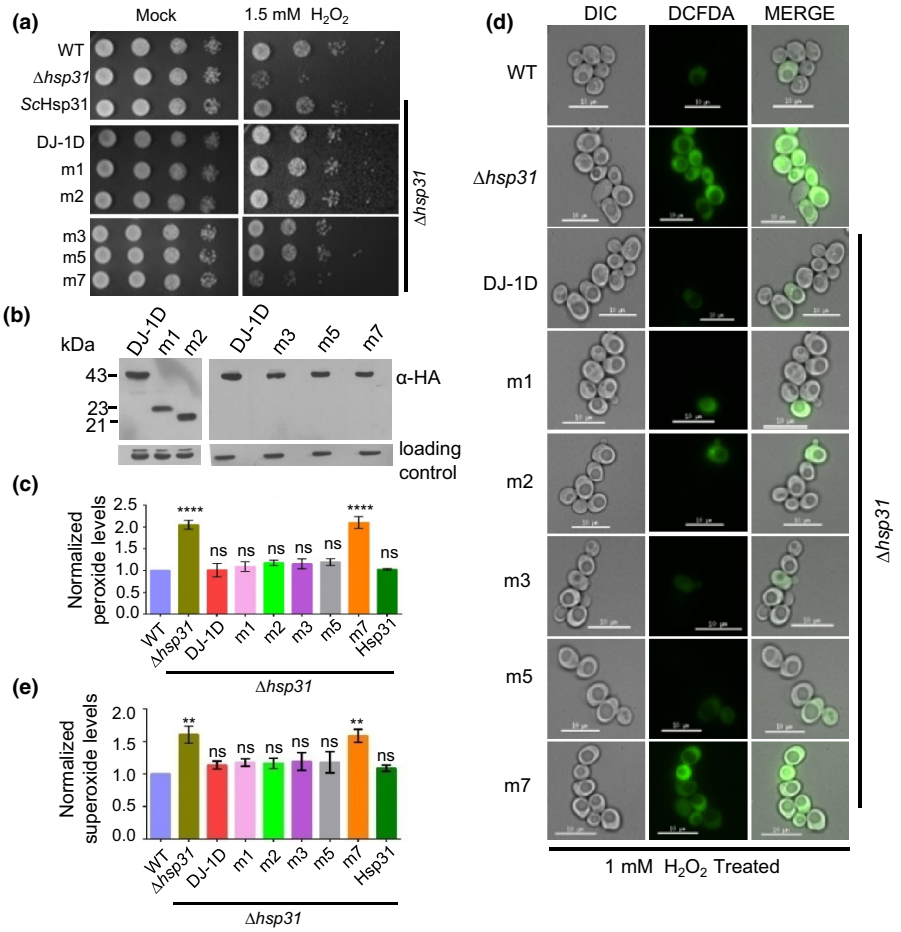

Fig. 4 Expression of DJ-1D suppresses oxidative stress phenotype of yeast Δ*hsp31*. (a) Growth phenotype analysis showing DJ-1D provides H_2O_2 tolerance. Yeast cells from wild-type (WT), Δ*hsp31*- and Δ*hsp31*-overexpressing DJ-1D and its mutants were subjected to spot analysis in the absence (left) and presence of 1.5 mM H_2O_2 (right) on SD Leu$^-$ media. The growth rescue was monitored up to 42 h. (b) Western blot analysis showing the expression of DJ-1D and its mutants (upper panel). Immunodecoration with YDJ-1 specific antibody served as internal loading control (lower panel). (c) Assessment of cytosolic peroxide concentrations by flow cytometry analysis. Equivalent amounts of cells from each strain were subjected to 1.5 mM H_2O_2 treatment and stained with H_2DCFDA followed by flow cytometry. Data from three representative experiments are shown (mean ± SE; one-way ANOVA: **, $P \leq 0.01$; ****, $P \leq 0.0001$; ns, not significant). (d) Fluorescence imaging analysis showing H_2DCFDA-stained cells from the WT and *Δhsp31*, *Δhsp31*/ DJ-1D and *Δhsp31*/ DJ-1D mutant strains after treatment with 1 mM H_2O_2 by Delta Vision Elite microscope using a ×100 objective lens. Bar, 10 μm. The cells in all the panels were imaged at identical exposures to compare the fluorescence intensities. (e) Assessment of cytosolic superoxide concentrations by flow cytometry analysis using dihydroxyethidium dye.

seen in expression analysis using the anti-HA antibody (Fig. S6b). However, expression of m1 and m2 under stronger GPD promoter suppressed the growth sensitivity against H_2O_2 stress (Fig. 4b). Conversely, the complementation of m7, which is deficient in its methylglyoxalase activity, was unable to rescue the growth, unlike the DJ-1D and other mutants under the equal level of protein expression (Fig. 4a,b).

To further confirm these redox-sensing activities of DJ-1D, we measured the cytosolic concentrations of free radicals using H_2-DCFDA and dihydroxyethidium dye staining which aid in measuring total cellular ROS and cellular superoxide concentrations, respectively. In agreement with the activities described earlier, flow cytometry measurements revealed restoration of redox homeostasis by DJ-1D and its mutants (m1, m2, m3 and m5) in Δ*hsp31* background, similar to the levels seen with *Sc*Hsp31 (Fig. 4c; Methods S4). This was further supported by the total cellular ROS measurements using microscopy, in which fluorescence of the Δ*hsp31* strain was significantly suppressed upon expression of DJ-1D or its mutants (Fig. 4d (compare DCFDA panels 2 with 3–7); Methods S4). Similarly, DJ-1D and its mutants significantly reduced cellular superoxide concentrations in the Δ*hsp31* strain (Fig. 4e). However, in contrast, m7 mutant was unable to restore both the total cellular ROS and superoxide concentrations in Δ*hsp31* cells (Figs 4c,d (last panel), 4e), thus demonstrating the role of conserved cysteine of DJ-1 family members in ROS homeostasis. In summary, these results provide compelling evidence for the critical nature of DJ-1D and its individual domains in regulating redox homeostasis.

Transgenic plants expressing DJ-1D provide tolerance to abiotic stresses

To investigate the physiological implications of DJ-1D *in planta*, we generated *Arabidopsis* transgenic plants overexpressing DJ-1D (DJ-1D_OE) driven by constitutive CaMV 35S promoter (Fig. S7a). We obtained multiple independent DJ-1D_OE transgenic plants (Fig. S7a) with high expression of transgene, both at the RNA (Fig. S7b; Methods S1) and protein levels (Fig. S7c). We observed that DJ-1D_OE plants have significantly higher expression of DJ-1D (three- to five-fold) compared with the control Col-0 plants (Fig. S7d). Interestingly, the DJ-1D_OE plants showed robust growth phenotype (Figs 5a, S7a,e), including broad and longer leaves when compared with the control (Figs 5b, S7f). We further explored whether DJ-1D-expressing transgenic plants have high stress tolerance similar to that of yeast Hsp31-overexpressing transgenic plants, as we observed previously (Melvin *et al.*, 2017). Under MG stress, 6-wk-old transgenic plants had reduced accumulation of MG-induced AGEs in DJ-1D_OE plants compared with control plants (Fig. 5c). To determine whether methylglyoxalase activity was responsible

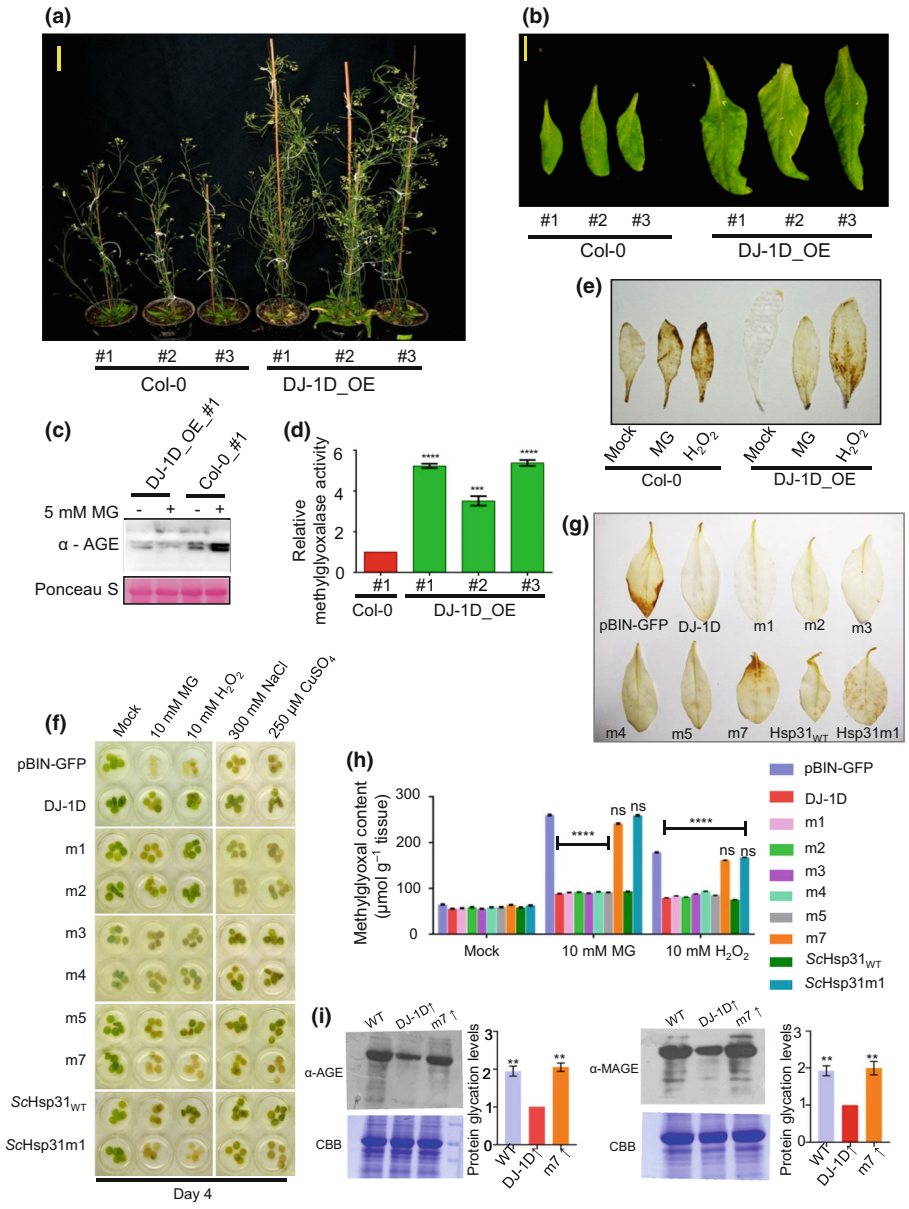

Fig. 5 DJ-1D offers stress tolerance in transgenic plants. (a) Phenotypic features of *Arabidopsis* wild-type (Col-0) and transformants expressing DJ-1D_eGFP (DJ-1D_OE); representative shoots of mature plants (6 wk old). Bar, 5 cm. (b) Representative leaves of *Arabidopsis* wild-type (Col-0) and transformants expressing DJ-1D_eGFP plants (6 wk old). Bar, 1 cm. (c) DJ-1D reduces formation of advanced glycated end-products (AGE). Total protein was isolated from mock and MG-stressed (5 mM) 6-wk-old *Arabidopsis* Col-0 and DJ-1D_OE-expressing plants, and immunoblot was carried with anti-AGE antibody. (d) Methylglyoxalase activity of the 6-wk-old *Arabidopsis* Col-0 and DJ-1D_OE-expressing plants. (e) Reactive oxygen species (ROS) accumulation in *Arabidopsis* Col-0 and DJ-1D_OE-expressing plants (6 wk old) exposed to 5 mM MG and 10 mM H_2O_2 by DAB staining. (f) DJ-1D overexpression in transgenic tobacco offers stress tolerance. Leaf disks from transgenic tobacco plants were incubated for 4 d with stress inducers (10 mM MG, 10 mM H_2O_2, 300 mM NaCl and 250 μM $CuSO_4$). (g) Reactive oxygen species accumulation in transgenic plants exposed to 300 mM NaCl by DAB staining. (h) MG content in tobacco plants under MG and H_2O_2 stress. (i) Determination of AGE and MG-induced AGE (MAGE) from transgenic tobacco plants by probing with anti-AGE and anti-MAGE antibody. CBB was used as loading control. Graphs represents the protein glycation levels in the respective transgenic tobacco plants (error bars are means ± SE; one-way ANOVA: **, $P \leq 0.01$; ***, $P \leq 0.001$; ****, $P \leq 0.0001$; ns, not significant).

for the reduction in AGE accumulation, we measured methylglyoxalase activity in the tissue extracts derived from DJ-1D_OE and control plants. As expected, DJ-1D_OE-derived extract had enhanced methylglyoxalase activity as compared with Col-0 (Fig. 5d; Methods S3). Enhanced growth and stress tolerance correlated with reduced accumulation of ROS in DJ-1D_OE plants (Fig. 5e). These results show that overexpression of DJ-1D suppresses MG-induced cellular damage, leading to robust growth and tolerance to stress. Repeated attempts to generate *Arabidopsis* knockdown plants of DJ-1D were not successful, indicating the importance of this gene in plant growth and development.

To test if the presence of the double DJ-1 domain in DJ-1D is beneficial in mediating stress tolerance, we generated binary vector constructs (Figs 1b, S8) to express either full-length or truncated or mutated versions of DJ-1D. All these constructs had DJ-1D or its variants driven by the CaMV 35S promoter. Transgenic plants were generated using the tobacco model system which is amenable to various transient and stress assays. Multiple transgenic plants expressing high levels of DJ-1D or its deletion and mutant versions were obtained (Fig. S9a), among which highly and uniformly expressing transgenes were selected for further analysis (Fig. S9b). We observed a slightly higher accumulation of total Chl content in the transgenic plants expressing DJ-1D and its mutants (m1, m2, m3, m4, m5) which were comparable to the transgenic plants expressing yeast Hsp31 included as a positive control (Melvin *et al.*, 2017). However, the Chl content in plants expressing m7 was similar to that in nontransgenic plants (Fig. S9c). To further assess the functional relevance of DJ-1D in mediating abiotic stress tolerance, we challenged leaves with various stresses (such as 10 mM MG, 10 mM H_2O_2, 300 mM NaCl, 250 μM $CuSO_4$ or 40% polyethylene glycol). The tobacco leaf disks expressing 35S:GFP served as control (VC). After 4 d of

treatment with stress inducers, we observed that leaf disks derived from plants expressing DJ-1D, m1, m2, m3, m4 and m5 showed tolerance against all the tested stresses as compared with the VC (Figs 5f, S10a–f). Unlike the results described earler, no distinguishable difference in tolerance was observed among m1, m2, m3, m4 and m5. Interestingly, we observed that plants expressing m7 exhibited susceptibility to a degree seen in VC or Hsp31m1 (Fig. 5f). These results were validated by quantifying changes in the Chl content (Fig. S10b,f). By contrast, VC and m7 plants displayed a pale yellow appearance as a result of damage induced by stresses (Figs 5f, S10a–d). Quantitative DW measurements provided further support for these observations (Fig. S10a,e).

To explore how exactly DJ-1D mediated stress tolerance in plants, we evaluated the activity of DJ-1D in reducing or alleviating the stress-induced harmful effects. To check the extent of cellular injury during abiotic stress conditions, the accumulation of toxic MG, MDA and ROS concentrations was measured in stress-exposed VC and DJ-1D-expressing plants. Accumulation of toxic MG, MDA and ROS in MG- and H_2O_2-exposed transgenic plants indicated high MG and lipid peroxidation and stronger DAB staining in m7 than in plants expressing DJ-1D and mutants m1, m2, m3, m4 or m5 (Figs 5g,h, S10c; Methods S5), indicating that DJ-1D probably prevents formation of these molecules. We also measured endogenous levels of different genes coding for antioxidant and defense genes such as cytochrome oxidase (COX6), catalase (CAT1), ascorbate peroxidase (APX6), superoxide dismutase (CSD1) and peroxidase (PER12) in transgenic lines subjected to different abiotic stresses (such as 10 mM MG and 10 mM H_2O_2; Fig. S10g; Table S2; Methods S1). The normalized levels of antioxidant responsive genes (COX6, CAT1, CSD1, PER12 and PR1) were higher (more than two-fold) in plants expressing DJ-1D WT than in the VC. Plants expressing m7 had similar RNA levels to those of the VC. However, we did not observe significant changes in the expression of APX6. The activities of CSD1, COX6, CAT1, PER12 and PR1 increased rapidly in stress-treated DJ-1D transgenic plants as compared with VC or m7 plants (Fig. S10g). These enzymes are essential for the rapid scavenging of cell-damaging ROS molecules. Moreover, under MG stress, DJ-1D transgenic plants had reduced accumulation of AGEs and MAGEs compared with control and DJ-1D m7 transgenic plants (Fig. 5i).

DJ-1D localizes to mitochondria under stress and repairs MG-induced DNA lesions

DJ-1 proteins are known to translocate to mitochondria during stress conditions in humans and yeast (Canet-Avilés *et al.*, 2004; Bankapalli *et al.*, 2015). *Sc*Hsp31 also translocated to mitochondria(mt) under stress in transgenic plants (Melvin *et al.*, 2017). In transgenic leaves, green fluorescent protein (GFP)-tagged DJ-1D was localized in both mitochondria and cytoplasm; however, we also observed its localization in the cell periphery. Upon induction of stress, there was an increase in localization of DJ-1D_eGFP in mitochondria and nucleus in three independent experiments (Fig. S11a–c; Methods S6). To further support this observation, we performed immunoblot analysis of the purified mitochondria, derived from transgenic DJ-1D_eGFP-overexpressing plants treated with 5 mM H_2O_2. We observed a significant enrichment of DJ-1D in mitochondria during oxidative stress as compared with controls (Fig. 6a). ATP synthase (ATPβ) was used as a positive control. The absence of other marker proteins, such as histone H4 (nuclear) and actin (cytosol), was used to ascertain the purity of the mitochondria (Fig. 6a; Methods S2). In parallel, we also isolated nuclei from control and 5 mM H_2O_2-treated DJ-1D_eGFP transgenic plants and observed enhanced DJ-1D protein levels in nuclei fractions derived from treated plants (Fig. 6b). Similar to yeast Hsp31 (Melvin *et al.*, 2017), the qRT-PCR analysis showed significant induction in the expression of mt-encoded genes such as COX1, MRP, DPH and NADH dehydrogenase in stressed DJ-1D transgenic plants (Fig. 6c).

As DJ-1D is capable of repairing glycated DNA, we speculated that it might rescue mutations in mitochondrial (mt) DNA under stress. Murata-Kamiya *et al.* (2000) showed that MG induced G:C to C:G and G:C to T:A transversions in the mammalian *supF* gene. It is also well known that glyoxals can induce spontaneous mutations (Kawanishi *et al.*, 2014). Amplification and analysis of COX1, MRP, DPH and NDH2 genes through Illumina next-generation sequencing indicated higher mutations under MG stress that are rescued by the expression of WT DJ-1D but not its mutant m7 (Figs 6d, S12a–d). Specifically, higher rates of G:C to A:T and G:C to T:A transversions were observed in mt genes (Figs 6d–f, S12a–d). Similar results were observed in yeast cells expressing DJ-1D. Yeast cells lacking *glo1* and the *glo1* complemented with m7 showed mutations in the COX2 gene under MG stress. Such mutations in DJ-1D-complemented Δ*glo*1 yeast cells were not observed (Fig. S13a). Together these results indicate the importance of DJ-1D in macromolecular protection in general, and DNA repair in particular, against toxicity induced by reactive carbonyls.

Discussion

The plant genome evolves at a higher frequency than other eukaryotes as a result of constant environmental challenges, resulting in higher genome diversity (Murat *et al.*, 2012). A primary mechanism of genome diversity is attributed to a gene duplication event, which generates multiple copies of pre-existing genes (Flagel & Wendel, 2009). Such a phenomenon has a broad application in adaptive evolution, particularly in combating diverse stress conditions.

Our comprehensive survey of DJ-1 members in a wide range of taxonomically diverse species suggests a high copy number of DJ-1 paralogs in *Plantae* compared with other prokaryotic and eukaryotic species. Interestingly, evolutionary studies indicate that about 65% of plant genes have paralogs mainly involved in signal transduction, stress response and transcriptional regulation (Panchy *et al.*, 2016), which explains the presence of multiple DJ-1 paralogs in the plant kingdom. Our phylogenetic analysis also highlights a greater abundance of DJ-1 paralogs in angiosperms (monocots and dicots), which might have contributed to speciation and diversification of angiosperms. The *A. thaliana*

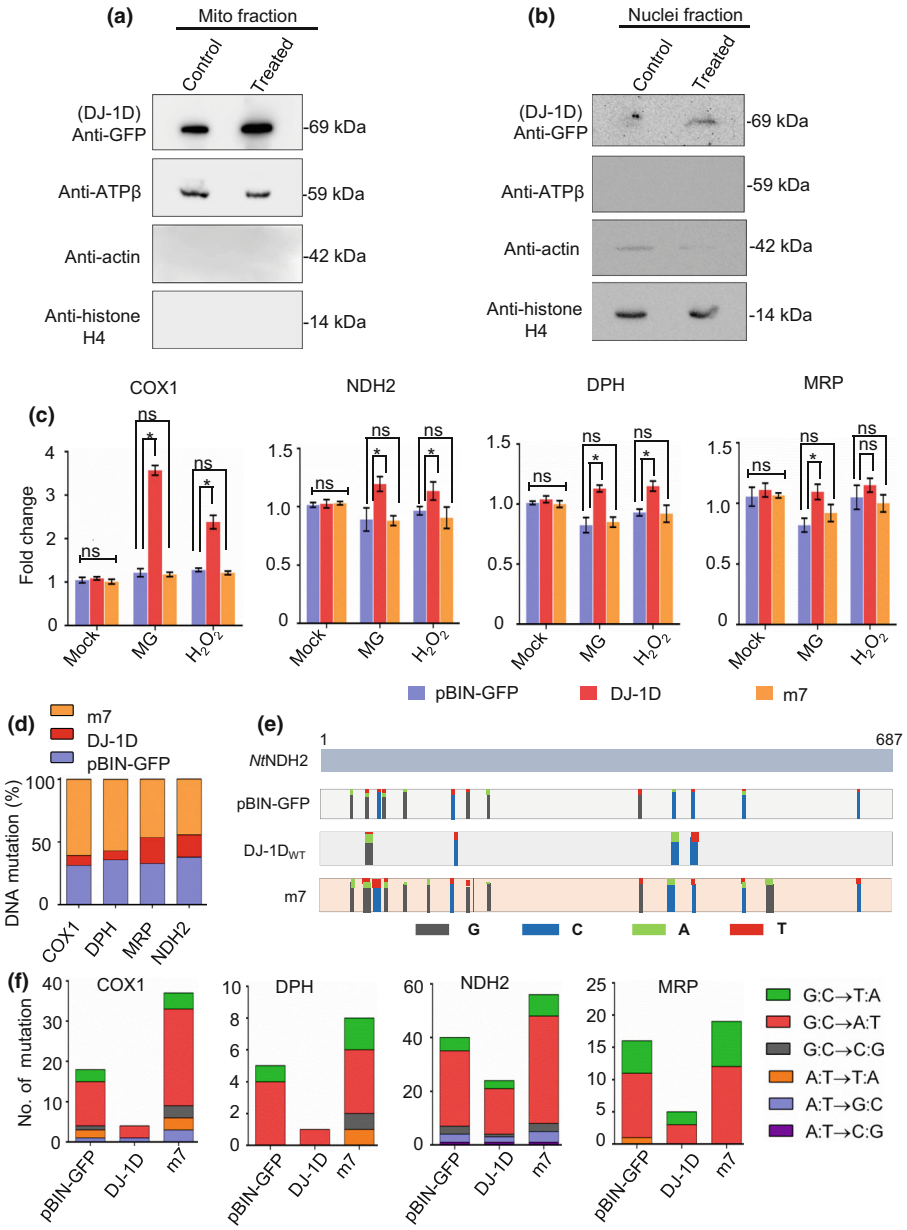

Fig. 6 DJ-1D repairs methylglyoxal (MG)-induced mitochondrial DNA lesions. (a, b) Localization of DJ-1D_eGFP was tested in purified mitochondria (a) and nuclei (b) from control (untreated) and 5 mM H_2O_2-treated transgenic tobacco plants by immunoblotting with anti-GFP antibody. ATPβ and histone H4 were used as mitochondrial and nucleus controls, respectively. Actin was used as cytosolic control. (c) Quantitative real-time PCR analysis of mitochondria-specific genes in vector control, DJ-$1D_{WT}$ and m7 under MG and H_2O_2 stress. Values are normalized to *GAPDH* expression. Schematic representation of the position of mutations induced by MG in COX1, DPH, MRP and NDH2 genes is shown. The values are means ± SD from three independent experiments (error bars represent means ± SE; one-way ANOVA: *, $P \leq 0.05$; **, $P \leq 0.01$; ns, not significant). (d) Mutations in COX1, NDH2, DPH and MRP genes in plants expressing DJ-1D or its mutants under MG stress. (e) Schematic representation of the position of mutations in the NDH2 (NADH dehydrogenase) gene in stress-induced tobacco plants. (f) Types of mutation in COX1, NDH2, DPH and MRP genes.

model plant possesses six DJ-1 members with varying sequence diversity and expression among different plant parts. We show that *At*DJ-1D has the highest expression among the paralogs in the tissues tested. Such differential expression of paralogs has also been reported in *Oryza sativa*, where *Os*DJ-1C and *Os*DJ-1E exist in high transcript abundance (Ghosh *et al.*, 2016), probably as a result of strong positive selection pressure and functional allocation owing to sequence divergence.

Besides having multiple gene copies, the majority of the plant DJ-1 proteins contain two DJ-1 domains tandemly arranged within a single polypeptide backbone, making a pseudo-dimeric protein. The domain fusion property of DJ-1 members is observed in a few species of green algae and found in the rest of the plant kingdom (Fig. S1). This striking observation could result from a change in habitat from aquatic to terrestrial, along with altered environmental conditions. *Arabidopsis* DJ-1 members also display double domain nature, particularly *At*DJ-1D, which contains overlapping sequences with *Sc*Hsp31 and hDJ-1, further amplifying its physiological role. The fusion of both domains provided significantly higher methylglyoxalase activity to *At*DJ-1D than to hDJ-1 and *Sc*Hsp31, and this function is physiologically advantageous to the plants (Lee *et al.*, 2012; Kwon *et al.*, 2013; Bankapalli *et al.*, 2015). Notably, the individual domains of DJ-1D (m1 and m2) and their cysteine/histidine mutants (m3–m6) also efficiently scavenged MG. However, mutations in both domains (m7) altogether abolished the activity, suggesting that one catalytically active functional domain is sufficient for survival.

The endogenous concentrations of MG are highly influenced by various environmental factors such as daylight to dark growth cycle and diurnal period, resulting in aberrant glycation of vital biomolecules (Bechtold *et al.*, 2009). Glycation at a higher rate

leads to compromised plant vitality and early senescence, affecting the gross yield of crops. The detoxification of MG in plants is primarily driven by the glyoxalase system (GLOI and II) by utilizing glutathione (GSH) as a cofactor. However, under stress conditions, the concentrations of GSH are compromised. Therefore, despite a stringent glyoxalase system, we observed enhanced glycation of macromolecules along with a spectrum of mutations in several genes. This is primarily a result of the limitation of the GSH pool, making the glyoxalase system (GLOI and II) inefficient to scavenge excess carbonyls. By contrast, having DJ-1D (glyoxalase III) is highly beneficial to the system as it efficiently detoxifies MG without utilizing GSH (Fig. 7). At the same time, the DJ-1D also alleviates the proteome glycation and mutation frequency while maintaining the GSH homeostasis (Bankapalli *et al.*, 2015). Besides maintaining carbonyl homeostasis, DJ-1D also repairs the glycation adducts of nucleic acids and proteins (Fig. 7), further emphasizing the critical requirement of DJ-1D during dicarbonyl stress. Interestingly, a mutation in either single domain does not affect the deglycase activity of DJ-1D, unlike mutations in both the domains, suggesting the pivotal role of catalytic cysteines for overall function.

Our findings further support the deglycase activity of DJ-1 superfamily proteins reported earlier, which are involved in a novel glycation repair pathway in plants to restore and maintain integrity of genomes and proteomes. Various environmental stresses elicit misfolding and aggregation of proteins, leading to proteotoxic stress, which is significantly attenuated through a complex network of molecular chaperones, including DJ-1 members (Shendelman *et al.*, 2004; Aslam & Hazbun, 2016). Our *in vitro* and *in vivo* studies in *S. cerevisiae* demonstrate that *At*DJ-1D is a robust chaperone that prevents amyloid formation induced by various substrates (rhodanese and hSOD1 H46R) and functions in regulating proteostasis. Glycation of proteins has been reported to promote protein aggregation and amyloid formation. Mechanistically, the deglycase property of DJ-1D could involve the chaperone activity that allows binding or gaining access to glycated macromolecules, as proposed earlier (Richarme *et al.*, 2015).

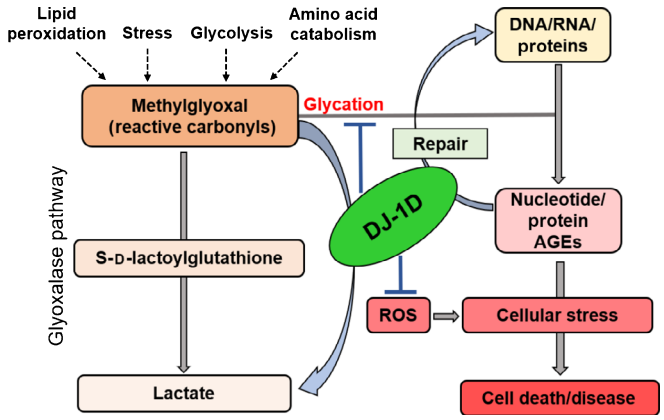

Fig. 7 Model illustrating how DJ-1D protects macromolecules from methylglyoxal (MG)-induced cytotoxicity. The reactive carbonyl species like MG generated through various distressed metabolic pathways induce macromolecule glycation, resulting in higher accumulation of advanced glycation end-products (AGEs), which leads to cellular stress and cell death. DJ-1D is a multifunctional protein that possesses methylglyoxalase and macromolecular deglycation repair abilities. It also reduces glycation damage and provides oxidative stress resistance. ROS, reactive oxygen species.

Lower threshold concentrations of MG trigger ROS, calcium signaling and abscisic acid phytohormone accumulation. At the same time, the elevation of MG is invariably associated with altered redox homeostasis and oxidative damage (Hoque *et al.*, 2016). The leaves of *Arabidopsis*- and *Nicotiana*-overexpressing DJ-1D and its mutants provided higher Chl retention and enhanced tolerance towards oxidative stress. Additionally, plants exposed to various abiotic stresses such as metals, salinity and osmotic stress led to the production of MG (Hossain *et al.*, 2009) and H_2O_2, whose deleterious effects may result in chlorosis, necrosis, stunting and senescence. Our comprehensive study using transgenic plants overexpressing DJ-1D and its mutants provided multi-stress tolerance, probably by scavenging MG and H_2O_2 (Fig. 7). Importantly, DJ-1D localized into mitochondria and nucleus to provide enhanced organellar protection during various abiotic stresses, enabling plants to survive in harsher environmental conditions.

In conclusion, this study explains how a gene-fusion event mediates tolerance to multiple stresses in plants. Here, we report a novel glycation repair pathway in plants that enables the maintenance and repair of macromolecules during dicarbonyl stress. As we also observed a superior growth of transgenic plants along with broader leaves in the presence of DJ-1D, it is an exciting candidate for engineering in yield improvement and stress tolerance. Deciphering the physiological role of DJ-1 members in various plants can provide better insights into the adaptation and fitness of plants.

Acknowledgements

We thank Prof. Elizabeth A. Craig (University of Wisconsin–Madison, Madison, WI) for gifting yeast plasmids and antibodies against YDJ-1. We thank Prof. Chandan Sahi (Biological Sciences, IISER Bhopal) for gifting ATPβ antibody. We thank Dr Nargis Parvin (Department of Microbiology and Cell Biology, IISc Bangalore) for assisting with mitochondrial isolation from plants. We thank C.Y. Harshith for helping with plant materials. We thank the NCBS-TIFR for use of its Next Generation Genomics, CIFF, mass-spectrometry, radiation and glasshouse facilities, and IISc, Bangalore, for use of the FACS-facility. PVS's laboratory is supported by NCBS-TIFR core funding (DAE RTI 4006) and grants (BT/IN/Swiss/47/JGK/2018-19; BT/PR25767/GET/119/151/2017) from the Department of Biotechnology, Government of India. PDS acknowledges financial support from a DST-SERB grant (CRG/2018/001988), the Department of Biotechnology (DBT-IISc Partnership Program Phase-II, no. BT/PR27952/IN/22/212/2018), and the DST-FIST Program-Phase III (no. SR/FST/LSII-045/2016-G). MP acknowledges a DBT-Research Associateship, DBT, Government of India. PK and GS acknowledge fellowships from IISc. SN acknowledges a postdoctoral fellowship from SERB (PDF/2015/000157N-PDF).

Competing interests

None declared.

Author contributions

PVS and PDS designed the study, provided resources, analyzed the data and obtained funding. MP and PK performed and analyzed experiments. SN purified proteins and performed glyoxalase analysis. GS performed deglycase analysis. KB conducted microscopy analysis. RB, MP and RV performed HPLC analysis. CS performed NGS data analysis. PVS, MP and PK wrote the manuscript with input from PDS. MP and PK contributed equally to this work.

ORCID

Kondalarao Bankapalli https://orcid.org/0000-0002-0278-0931
Patrick D'Silva https://orcid.org/0000-0002-1619-5311
Priyanka Kataria https://orcid.org/0000-0003-1860-4286
Sunayana Ningaraju https://orcid.org/0000-0003-4295-4841
Melvin Prasad https://orcid.org/0000-0002-3925-1398
Padubidri V. Shivaprasad https://orcid.org/0000-0002-9296-4848
Gautam Susarla https://orcid.org/0000-0002-3798-749X
Chenna Swetha https://orcid.org/0000-0002-9336-0798
Radhika Venkatesan https://orcid.org/0000-0002-8112-9505

Data availability

The data that support the findings of this study are available in the Supporting Information of this article. Next-generation sequencing data of PCR fragments used in Fig. 6 are deposited in NCBI-SRA; the accession number is BioProject ID PRJNA859641.

References

Abdallah J, Mihoub M, Gautier V, Richarme G. 2016. The DJ-1 superfamily members YhbO and YajL from *Escherichia coli* repair proteins from glycation by methylglyoxal and glyoxal. *Biochemical and Biophysical Research Communications* **470**: 282–286.

Ahmed N, Battah S, Karachalias N, Babaei-Jadidi R, Horányi M, Baróti K, Hollan S, Thornalley PJ. 2003. Increased formation of methylglyoxal and protein glycation, oxidation and nitrosation in triosephosphate isomerase deficiency. *Biochimica et Biophysica Acta (BBA) – Molecular Basis of Disease* **1639**: 121–132.

Aslam K, Hazbun TR. 2016. Hsp31, a member of the DJ-1 superfamily, is a multitasking stress responder with chaperone activity. *Prion* **10**: 103–111.

Atamna H, Cheung I, Ames BN. 2000. A method for detecting abasic sites in living cells: age-dependent changes in base excision repair. *Proceedings of the National Academy of Sciences, USA* **97**: 686–691.

Bankapalli K, Saladi S, Awadia SS, Goswami AV, Samaddar M, D'Silva P. 2015. Robust glyoxalase activity of Hsp31, a ThiJ/DJ-1/PfpI family member protein, is critical for oxidative stress resistance in *Saccharomyces cerevisiae*. *Journal of Biological Chemistry* **290**: 26491–26507.

Bechtold U, Rabbani N, Mullineaux PM, Thornalley PJ. 2009. Quantitative measurement of specific biomarkers for protein oxidation, nitration and glycation in Arabidopsis leaves. *The Plant Journal* **59**: 661–671.

Canet-Avilés RM, Wilson MA, Miller DW, Ahmad R, McLendon C, Bandyopadhyay S, Baptista MJ, Ringe D, Petsko GA, Cookson MR. 2004. The Parkinson's disease protein DJ-1 is neuroprotective due to cysteine-sulfinic acid-driven mitochondrial localization. *Proceedings of the National Academy of Sciences, USA* **101**: 9103–9108.

Cannan WJ, Pederson DS. 2016. Mechanisms and consequences of double-strand DNA break formation in chromatin. *Journal of Cellular Physiology* **231**: 3–14.

Cao J, Lou S, Ying M, Yang B. 2015. DJ-1 as a human oncogene and potential therapeutic target. *Biochemical Pharmacology* **93**: 241–250.

Chatterjee N, Walker GC. 2017. Mechanisms of DNA damage, repair, and mutagenesis. *Environmental and Molecular Mutagenesis* **58**: 235–263.

Davie CA. 2008. A review of Parkinson's disease. *British Medical Bulletin* **86**: 109–127.

Flagel LE, Wendel JF. 2009. Gene duplication and evolutionary novelty in plants. *New Phytologist* **183**: 557–564.

Ghosh A, Kushwaha HR, Hasan MR, Pareek A, Sopory SK, Singla-Pareek SL. 2016. Presence of unique glyoxalase III proteins in plants indicates the existence of shorter route for methylglyoxal detoxification. *Scientific Reports* **6**: 1–15.

Goswami AV, Chittoor B, D'Silva P. 2010. Understanding the functional interplay between mammalian mitochondrial Hsp70 chaperone machine components. *Journal of Biological Chemistry* **285**: 19472–19482.

Hoque TS, Hossain MA, Mostofa MG, Burritt DJ, Fujita M, Tran L-SP. 2016. Methylglyoxal: an emerging signaling molecule in plant abiotic stress responses and tolerance. *Frontiers in Plant Science* **7**: 1341.

Hossain MA, Hossain MZ, Fujita M. 2009. Stress-induced changes of methylglyoxal level and glyoxalase I activity in pumpkin seedlings and cDNA cloning of glyoxalase I gene. *Australian Journal of Crop Science* **3**: 53.

Kawanishi M, Matsuda T, Yagi T. 2014. Genotoxicity of formaldehyde: molecular basis of DNA damage and mutation. *Frontiers in Environmental Science* **2**: 36.

Kwon K, Choi D, Hyun JK, Jung HS, Baek K, Park C. 2013. Novel glyoxalases from *Arabidopsis thaliana*. *The FEBS Journal* **280**: 3328–3339.

Lee J, Song J, Kwon K, Jang S, Kim C, Baek K, Kim J, Park C. 2012. Human DJ-1 and its homologs are novel glyoxalases. *Human Molecular Genetics* **21**: 3215–3225.

Lin J, Nazarenus TJ, Frey JL, Liang X, Wilson MA, Stone JM. 2011. A plant DJ-1 homolog is essential for *Arabidopsis thaliana* chloroplast development. *PLoS ONE* **6**: e23731.

Melvin P, Bankapalli K, D'Silva P, Shivaprasad PV. 2017. Methylglyoxal detoxification by a DJ-1 family protein provides dual abiotic and biotic stress tolerance in transgenic plants. *Plant Molecular Biology* **94**: 381–397.

Miller-Fleming L, Antas P, Pais TF, Smalley JL, Giorgini F, Outeiro TF. 2014. Yeast DJ-1 superfamily members are required for diauxic-shift reprogramming and cell survival in stationary phase. *Proceedings of the National Academy of Sciences, USA* **111**: 7012–7017.

Murashige T, Skoog F. 1962. A revised medium for rapid growth and bio assays with tobacco tissue cultures. *Physiologia Plantarum* **15**: 473–497.

Murat F, Van de Peer Y, Salse J. 2012. Decoding plant and animal genome plasticity from differential paleo-evolutionary patterns and processes. *Genome Biology and Evolution* **4**: 917–928.

Murata-Kamiya N, Kamiya H, Kaji H, Kasai H. 2000. Methylglyoxal induces G:C to C:G and G:C to T:A transversions in the supF gene on a shuttle vector plasmid replicated in mammalian cells. *Mutation Research/Genetic Toxicology and Environmental Mutagenesis* **468**: 173–182.

Nair DN, Prasad R, Singhal N, Bhattacharjee M, Sudhakar R, Singh P, Thanumalayan S, Kiran U, Sharma Y, Sijwali PS. 2018. A conserved human DJ1-subfamily motif (DJSM) is critical for anti-oxidative and deglycase activities of *Plasmodium falciparum* DJ1. *Molecular and Biochemical Parasitology* **222**: 70–80.

Oh SE, Mouradian MM. 2018. Cytoprotective mechanisms of DJ-1 against oxidative stress through modulating ERK1/2 and ASK1 signal transduction. *Redox Biology* **14**: 211–217.

Panchy N, Lehti-Shiu M, Shiu S-H. 2016. Evolution of gene duplication in plants. *Plant Physiology* **171**: 2294–2316.

Richarme G, Liu C, Mihoub M, Abdallah J, Leger T, Joly N, Liebart J-C, Jurkunas UV, Nadal M, Bouloc P. 2017. Guanine glycation repair by DJ-1/Park7 and its bacterial homologs. *Science* **357**: 208–211.

Richarme G, Mihoub M, Dairou J, Bui LC, Leger T, Lamouri A. 2015. Parkinsonism-associated protein DJ-1/Park7 is a major protein deglycase that

repairs methylglyoxal-and glyoxal-glycated cysteine, arginine, and lysine residues. *Journal of Biological Chemistry* **290**: 1885–1897.

Sharma N, Rao SP, Kalivendi SV. 2019. The deglycase activity of DJ-1 mitigates α-synuclein glycation and aggregation in dopaminergic cells: role of oxidative stress mediated downregulation of DJ-1 in Parkinson's disease. *Free Radical Biology and Medicine* **135**: 28–37.

Shendelman S, Jonason A, Martinat C, Leete T, Abeliovich A, Zoghbi HY. 2004. DJ-1 is a redox-dependent molecular chaperone that inhibits α-synuclein aggregate formation. *PLoS Biology* **2**: e362.

Shimakawa G, Suzuki M, Yamamoto E, Saito R, Iwamoto T, Nishi A, Miyake C. 2014. Why don't plants have diabetes? Systems for scavenging reactive carbonyls in photosynthetic organisms. *Biochemical Society Transactions* **42**: 543–547.

Shivaprasad PV, Thillaichidambaram P, Balaji V, Veluthambi K. 2006. Expression of full-length and truncated Rep genes from Mungbean yellow mosaic virus-Vigna inhibits viral replication in transgenic tobacco. *Virus Genes* **33**: 365–374.

Skoneczna A, Miciałkiewicz A, Skoneczny M. 2007. *Saccharomyces cerevisiae* Hsp31p, a stress response protein conferring protection against reactive oxygen species. *Free Radical Biology and Medicine* **42**: 1409–1420.

Song L, Koga Y, Ecker JR. 2016. Profiling of transcription factor binding events by chromatin immunoprecipitation sequencing (ChIP-seq). *Current protocols in Plant Biology* **1**: 293–306.

Subedi KP, Choi D, Kim I, Min B, Park C. 2011. Hsp31 of *Escherichia coli* K-12 is glyoxalase III. *Molecular Microbiology* **81**: 926–936.

Thornalley PJ. 2008. Protein and nucleotide damage by glyoxal and methylglyoxal in physiological systems-role in ageing and disease. *Drug Metabolism and Drug Interactions* **23**: 125–150.

Thornalley PJ, Waris S, Fleming T, Santarius T, Larkin SJ, Winklhofer-Roob BM, Stratton MR, Rabbani N. 2010. Imidazopurinones are markers of physiological genomic damage linked to DNA instability and glyoxalase 1-associated tumour multidrug resistance. *Nucleic Acids Research* **38**: 5432–5442.

Tsai C, Aslam K, Drendel HM, Asiago JM, Goode KM, Paul LN, Rochet J-C, Hazbun TR. 2015. Hsp31 is a stress response chaperone that intervenes in the protein misfolding process. *Journal of Biological Chemistry* **290**: 24816–24834.

Veena, Reddy VS, Sopory SK. 1999. Glyoxalase I from *Brassica juncea*: molecular cloning, regulation and its over-expression confer tolerance in transgenic tobacco under stress. *The Plant Journal* **17**: 385–395.

Xie X, He Z, Chen N, Tang Z, Wang Q, Cai Y. 2019. The roles of environmental factors in regulation of oxidative stress in plant. *BioMed Research International* **2019**: 9732325.

Xin Z, Chen J. 2012. A high throughput DNA extraction method with high yield and quality. *Plant Methods* **8**: 26.

Xu XM, Lin H, Maple J, Björkblom B, Alves G, Larsen JP, Møller SG. 2010. The Arabidopsis DJ-1a protein confers stress protection through cytosolic SOD activation. *Journal of Cell Science* **123**: 1644–1651.

Zhang X, Henriques R, Lin S-S, Niu Q-W, Chua N-H. 2006. Agrobacterium-mediated transformation of *Arabidopsis thaliana* using the floral dip method. *Nature Protocols* **1**: 641–646.

Zheng Q, Omans ND, Leicher R, Osunsade A, Agustinus AS, Finkin-Groner E, D'Ambrosio H, Liu B, Chandarlapaty S, Liu S. 2019. Reversible histone glycation is associated with disease-related changes in chromatin architecture. *Nature Communications* **10**: 1–12.

Supporting Information

Additional Supporting Information may be found online in the Supporting Information section at the end of the article.

Fig. S1 Schematic representation of number of DJ-1 members in different plant, animal and fungal species and their domain architecture.

Fig. S2 Consensus phylogenetic tree of selected DJ-1 superfamily members.

Fig. S3 Sequence alignment of DJ-1 homologs.

Fig. S4 Analysis of methylglyoxalase activity of DJ-1D.

Fig. S5 Reversed-phase high-performance liquid chromatography analysis of glycated nucleotides.

Fig. S6 Expression of DJ-1D suppresses oxidative stress phenotype of yeast Δ*hsp31*.

Fig. S7 Phenotypic analysis of wild-type Arabidopsis Col-0 and DJ-1D_eGFP overexpressing plants.

Fig. S8 Schematic representation of the T-DNA DJ-1D constructs.

Fig. S9 Generation of transgenic tobacco plants.

Fig. S10 DJ-1D overexpressed tobacco plants alleviate lipid peroxidation and reactive oxygen species level under abiotic stress.

Fig. S11 Subcellular localization of DJ-1D.

Fig. S12 Methylglyoxal induces mutation in mitochondrial genes.

Fig. S13 Methylglyoxal induces mutation in yeast mitochondrial gene.

Methods S1 RNA extraction and quantitative RT-PCR analysis.

Methods S2 Protein purification and immunoblotting.

Methods S3 Methylglyoxalase activity assay.

Methods S4 Measurement of reactive oxygen species levels.

Methods S5 DAB staining for H_2O_2.

Methods S6 Transient expression and subcellular localization of DJ-1D.

Table S1 List of primers used for cloning DJ-1D and its derivatives in *Escherichia coli*, yeast and for qRT-PCR.

Table S2 List of primers used for the amplification of antioxidant and mitochondria-specific genes.

Table S3 DJ-1 proteins and their accession numbers.

Table S4 HPLC analysis of glycated dGTP.

Table S5 HPLC analysis of glycated GTP.

Please note: Wiley Blackwell are not responsible for the content or functionality of any Supporting Information supplied by the authors. Any queries (other than missing material) should be directed to the *New Phytologist* Central Office.